PROCEEDINGS, 42nd Workshop on Geothermal Reservoir Engineering
Stanford University, Stanford, California, February 13-15, 2017
SGP-TR-212

Fracture Mechanical Properties of Damaged and Hydrothermally Altered Rocks, Dixie Valley, NV: Implications for Fault Conduit Development in Geothermal Systems

Owen A. Callahan[1], Peter Eichhubl[2], Jon Olson[3], and Nicholas C. Davatzes[4]

1, 2 Bureau of Economic Geology, Jackson School of Geosciences, The University of Texas at Austin, Austin, TX, 78758

3 Department of Petroleum and Geosystems Engineering, The University of Texas at Austin

4 Earth and Environmental Sciences, Temple University

1 corresponding author: owen.callahan@gmail.com

Keywords: fracture mechanics, subcritical fracture growth, hydrothermal alteration

ABSTRACT

Enhanced water-rock interaction in hydrothermal systems changes the textural and mineralogical composition of host rock, affecting the mechanical properties of fault-fracture systems, their permeability structure, and thus the development of hydrothermal convection cells. To characterize the impact of alteration on fracture mechanical properties, we used double-torsion load-relaxation testing to measure subcritical fracture growth indices (SCI) and mode-I stress intensity at calculated fracture growth velocities of 10^{-6} m/s (K_{IC*}) in two sets of rock of varying chemical alteration from two different hydrothermal settings: a retrograde alteration assemblage dominated by chlorite-calcite-hematite, and an epithermal setting dominated by intense silicification. By comparing distinct hydrothermal alteration assemblages we can infer the relative changes in mechanical properties during progressive deformation and chemical alteration.

Our tests reveal that progressive alteration changes the fracture mechanical properties of the host rock, but that the type of alteration is more important than the alteration intensity. Increasing damage in the form of microcracks weakens the rock. However, silicification is associated with high K_{IC*} and SCI, implying it counteracts the impact of damage. Thus, a key control on the relative strength of altered rocks is the trade-off between the accumulation and preservation of damage versus the precipitation of minerals that heal these flaws.

Spatial variation in dominant alteration mechanisms across hydrothermal systems likely produces systematic changes in the mechanical properties of fault-fracture conduits and adjacent host rock. In the alteration assemblages that we sampled, precipitation in the shallow epithermal environment strengthens fault-fracture conduits, whereas unhealed damage and dissolution may contribute to mechanical localization of fault-fracture conduits at depth, producing a depth-dependent inversion in mechanical contrast between conduit and host rock.

1. INTRODUCTION

Many geothermal fields produce fluids from fractured reservoirs, but the development of such reservoirs is often hindered by the inherent complexity and heterogeneity of fracture networks. The influence of fault geometry on hydrothermal flow, with thermal anomalies and mineral deposits localized in dilational fault jogs, stepovers, or at fault tips, is well recognized (e.g. Curewitz and Karson, 1997; Eichhubl and Boles, 2000; Cox et al., 2001; Faulds et al., 2006; Anderson and Fairley, 2008; Eichhubl et al., 2009; Micklethwaite et al., 2010). Also well recognized are the chemical conditions that contribute additional levels of complexity, with dissolution, precipitation, and chemical alteration potentially changing the hydrologic properties of fault-facture networks (e.g. Facca and Tonani, 1967; Gheradi et al., 2007; Dempsey et al., 2012; Ord et al., 2012). Less well understood are the impacts of chemical alteration on the mechanical properties governing fracture growth and fracture network geometry themselves despite clear evidence indicating a complex relationship between mechanical evolution and chemical alteration (Sornette, 1999; Eichhubl et al., 2004, 2009; Davatzes and Hickman, 2010; Laubach et al., 2010; Finzi et al., 2011, Wyerling et al., 2014).

We hypothesize that changes in rock composition and texture, and resulting contrasts in fracture-mechanical properties between different alteration assemblages, are important to the organization of fracture-dominated conduits in hydrothermal systems. Although often neglected in mechanical characterization, fracture mechanical properties, such as mode-I fracture toughness and subcritical crack growth indices, help to describe the conditions necessary to cause brittle failure. Subcritical crack growth characterizes time-dependent failure and failure under sustained loads below peak loads. Subcritical crack growth has been invoked to help explain joint pattern development (Olson, 1993, 2004), the strength of faults, and the long-term brittle behavior of the crust (Anderson and Grew, 1977; Rudnicki et al., 1980; Brantut et al., 2013). However, only a limited number of subcritical indices have been reported for materials that realistically represent fault-zone material, which commonly contains significant damage and mineralogical changes resulting from hydrothermal alteration (e.g. Bruhn et al., 1994). We present experimental results from fracture mechanical testing of two pairs of hydrothermally altered samples, representing two different fault-hosted hydrothermal regimes. We demonstrate that chemical reactions, long recognized as important factors influencing the hydrologic properties of fault and fracture networks in hydrothermal systems, also impact the mechanical properties that govern fracture initiation, growth, and coalescence.

2. FRACTURE MECHANICS TESTING METHODS

We use double-torsion (DT) load relaxation tests to measure subcritical fracture growth index (SCI) and to obtain mode-I stress intensity (K_I) at a given crack velocity (K_{IC}*) after Rijken (2005) and Nara et al. (2012), which serves as an estimate of resistance to

mode-I fracture growth for these samples and a means of comparing fracture mechanical properties between samples. SCI relates the velocity of fracture propagation below the critical mode-I stress intensity factor to K_I by (Pletka and Wiederhorn, 1978):

$$V = V^*(K_I/K_0)^n \quad \text{Eq. 1}$$

where V is velocity, V^* is a constant, K_I is the mode-I stress intensity factor, K_0 is used to normalized K_I, and *n* is the subcritical index.

Double torsion tests are conducted on rock wafers with dimensions of 1.8 mm x 30 mm x 75 mm. Wafers are sliced from larger blocks and then ground to desired thickness using a thin sectioning machine. An axial guide groove, measuring ~0.5 mm deep, ~0.5 mm wide, and square in profile, is cut into the base of the wafer. Wafer dimensions are recorded with calipers to ~0.01 mm precision. Wafers that are uneven, cracked, or otherwise visibly flawed are not tested.

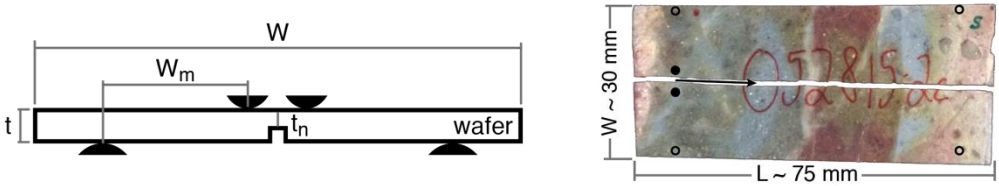

Figure 1. DT fracture mechanics wafer and loading schematic. The cross section on the left shows wafer dimensions, and the black semi-circles show loading points. The plan view on the right shows a fractured, post-test wafer and the relative position of lower supports (open circles) and loading ram points (closed circles). The black arrow shows fracture growth direction.

The DT testing apparatus consists of a base plate, ball bearings that function as wafer supports, a loading ram with internal force sensor, and a linear variable displacement transducer (LVDT) to record displacement. Load and displacement are recorded at a rate of ~5-8 samples per second. Wafers are placed in the DT apparatus with the axial guide groove facing down (after Pletka et al., 1979) and loaded from above using the loading ram. The wafer is placed in the DT apparatus so that the loading ram contacts the sample ~10 mm from the leading edge to reduce edge effects. Wafers are precracked by manual loading until a distinct load drop is observed. Subsequent loading occurs at a displacement rate between 1-2 μm/s. Loading is manually stopped when fracture propagation is indicated by a rapid drop in supported load. The load is then allowed to decay for 5-10 minutes. The test is complete when the wafer will no longer support a load, if more than ~7 load-decay curves are recorded, or if the sample fails catastrophically. All of our tests were conducted under ambient conditions at 23-24°C and relative humidity between 55 and 77%.

Ideal load-decay test patterns included a high pre-crack load (which is disregarded in later calculations), a subsequent plateau region of lower peak load and subsequent load decay curves that were used to calculate SCI and K_{IC*}, and a final load drop upon complete wafer failure (Figure 2). Among the samples tested, weaker materials commonly showed a decreasing stair step pattern after the initial peak, lacking the load plateau region. In these tests only the first post-precrack load was used to calculate SCI and K_{IC*}.

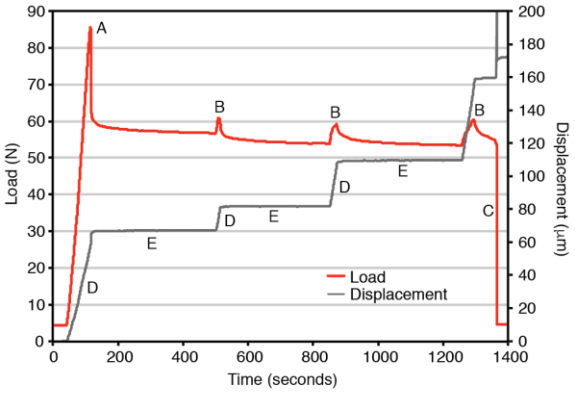

Figure 2. Ideal double torsion testing cycle consists of A) precrack load, B) subsequent loads in plateau region, C) load drop caused by crack acceleration to complete failure. Loads are driven by increasing displacement (D), and allowed to decay while displacement is held constant (E).

K_I is calculated from DT tests using the equation described in Williams and Evans (1973):

$$K_I = PW_m\sqrt{((3(1+\nu))/(Wt_nt^3))} \quad \text{Eq. 2}$$

where P is load during load-decay cycles, W_m is moment arm of the DT apparatus, ν is Poisson's ratio, W is wafer width, t is wafer thickness, and t_n is the reduced thickness along the axial groove (Figure 1). Poisson's ratios for fracture mechanics calculations (Eq. 2) were obtained from UCS tests using a GCTS rock mechanics system housed at the Rock Mechanics Lab at the Core Research Center,

Bureau of Economic Geology, Austin, TX. Some fracture mechanics wafers were obtained from smaller hand samples, and no material was available for elastic characterization; for these samples elastic properties were estimated from similarly altered and damaged samples.

The low loading rate that we used in these tests allowed for multiple load cycles and subcritical measurements from each wafer. However, low loading rates are not sufficient to accurately measure intrinsic fracture toughness due to the documented rate dependence of maximum supported load using the DT configuration (Evans, 1972). Consequently, we follow Rijken (2005) and Nara et al. (2012) and report relative stress intensity, K_{IC*}, at a given fracture growth velocity as a way to compare the toughness of different samples; we use 10^{-6} m/s from the calculated stress intensity-velocity (K-V) curves. Propagation velocity is calculated by fitting the load relaxation curve (Evans, 1972):

$$V = (-a_i P_i)/P^2(dP/dT) \quad \text{Eq. 3}$$

where a_i is initial fracture length and P_i is initial load at the start of each decay cycle, with an in house LabView script (Chen et al., in review).

3. SAMPLE SITES AND SAMPLE DESCRIPTIONS

Sample collection sites are located in Dixie Valley, NV, where Basin and Range faulting has localized modern hydrothermal activity and exhumed a variety of alteration assemblages. Sampling focused on two locations, the Dixie Comstock epithermal mine and the Box Canyons, that have notably different alteration histories and assemblages (Parry et al., 1991; Vikre, 1993; Bruhn et al., 1994; Hedderly-Smith, 1997). The Dixie Comstock site in central Dixie Valley contains anomalously high temperature alteration and mineralization in the shallow subsurface. At this location, moderately metasomatized mafic Jurassic plutonic units are overprinted by a variety of alteration assemblages, culminating in massive silicification, with some fault-parallel silicified breccia in excess of 2 m thick. Fluid inclusions in surface quartz veins record homogenization temperatures ~160-170°C (Vikre, 1993; Callahan, unpublished data). Relict or ghost calcite blades and the presence of liquid- and vapor-rich inclusions indicate boiling conditions in shallow parts of the system, and place depth estimates at <150 m (Haas, 1971). In contrast, alteration and fracturing at the Box Canyons site in southern Dixie Valley is dominantly retrograde, with early, deep, higher temperature alteration giving way to lower temperature assemblages during faulting and exhumation. At this location, reported alteration assemblages affecting Oligocene-Miocene plutonic units grade from early potassium feldspar-biotite to chlorite-epidote-calcite, with some areas recording additional sericite-quartz-kaolinite-smectite and zeolite alteration (Parry et al., 1991; Bruhn et al., 1994; Hedderly-Smith, 1997).

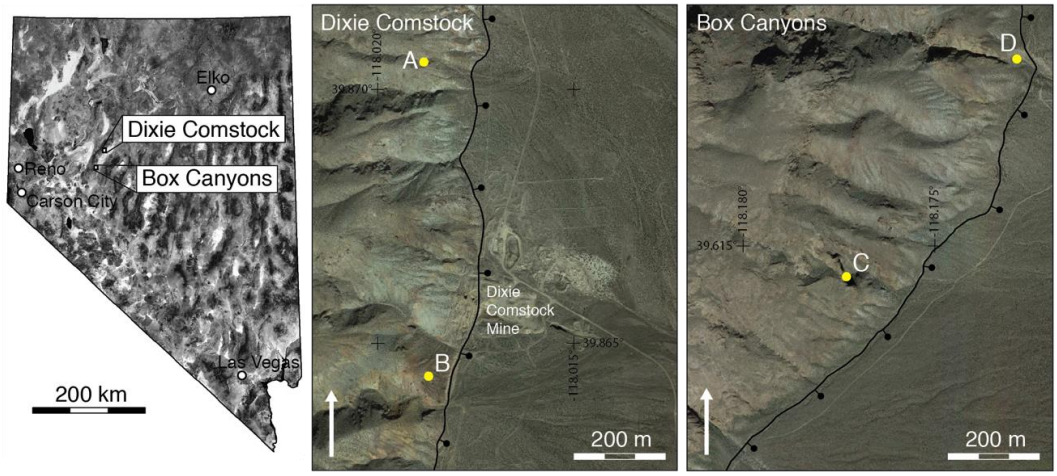

Figure 3. Samples were obtained from Dixie Comstock and the Box Canyons in Dixie Valley. Alteration at both sites is associated with Basin and Range normal faulting.

The Dixie Comstock samples were obtained from a distal portion of the footwall and from the silicified fault core (Samples A and B, Figure 3). Sample A (083114-2) is medium grained and dominated by plagioclase with minor quartz and secondary chlorite and epidote (Figure 4 A). Plagioclase exhibits minor sericitization and chloritization. Chlorite occasionally occurs with minor epidote. Quartz and plagioclase laths are broken, with no obvious porosity, and some sealing by chlorite and calcite. The silicified sample B (052815-2) is dominated by fine-grained, microquartz (Figure 4 B) which grades into chalcedony and euhedral quartz linings in fractures and vugs, with minor calcite, sulfides, and oxides. There is little observable porosity; open pore spaces are limited to quartz lined and nearly occluded vugs or incomplete fracture fill.

The Box Canyon samples were obtained from minimally altered diorite and from fault-proximal chlorite-calcite-hematite altered and damaged material (Samples C and D, Figure 3). Sample C (052615-1a) is composed of quartz, plagioclase, biotite, green amphibole, relict pyroxene, and minor hematite (Figure 4, C). Quartz grains contain minor deformation (patchy extinction, distinct extinction domains). Plagioclase laths contain minor sericite. Biotite and amphibole are relatively pristine. All crystals are intergrown, with little interstitial space. The mineralogy and primary texture of fault proximal Sample D (052615-2) are similar to the background sample but

Sample D contains more alteration and damage, with the addition of disseminated chlorite and calcite, quartz-chlorite-calcite-hematite filled fractures, and brecciation (Figure 4 D). Pervasive fracturing is accompanied by fragment rotation and grain size reduction of feldspars and quartz grains. Pre-existing fractures commonly follow feldspar cleavage and cut across grains. Effective maximum grain size is reduced to ~0.5 mm. Multiple cross cutting cataclastic bands, with micro- and euhedral quartz, disseminated calcite, chlorite, hematite, and crushed grains, are cut by thin, partially calcite- and hematite-filled fractures, recording multiple episodes of brittle deformation and cementation. Porosity is generally preserved in later, partially calcite-filled fractures, and along the edges of cataclastic bands.

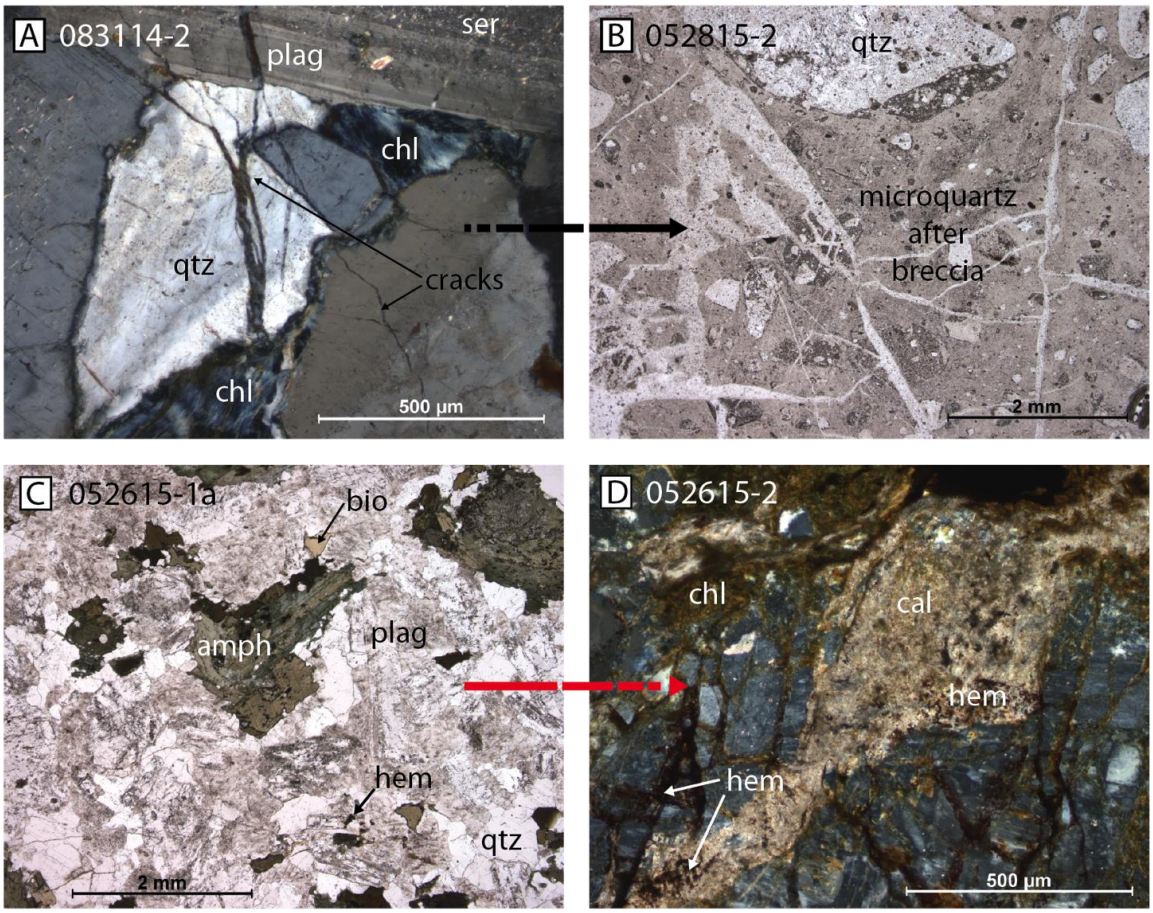

Figure 4. Photomicrographs of tested material. Dixie Comstock samples record progressive mineralization and silicification of fault proximal conduits, while the Box Canyon samples contain increasing damage near the fault zone. Chloritized and sericitized gabbro (A) in the footwall north of the Dixie Comstock mine contains partially mineralized cracks, while fault-proximal material adjacent to the main deposit records near complete replacement by microquartz (B). At the Box Canyons, background diorite (C) contains minimal alteration and only minor damage, while the fault proximal sample (D) contains chlorite, calcite, hematite alteration and abundant microfractures in quart and feldspar grains.

5. EXPERIMENTAL RESULTS

We present results from DT tests on 26 wafers from 4 samples. Some wafers failed before adequate testing and are not considered in these results. Basic sample statistics, including minimum, 25th quartile, median, mean, 75th quartile, and maximum values are shown in Table 1. The number of decay curves analyzed per sample ranged from 9-15. If the calculated K-V curves for any decay curve did not span the velocity of 10^{-6} m/s the relative stress intensity, K_{IC*}, was not calculated.

Table 1. Fracture Mechanical Results from Double Torsion Testing

Site	Sample		K_{IC*} @ 10^{-6} m/s (MPa√m)							SCI						
			Min	25%	Med	75%	Max	Mean	#	Min	25%	Med	75%	Max	Mean	#
DC	A	083114-2	0.18	0.46	0.76	0.88	1.02	0.67	13	36.8	43.7	50.7	58.2	83.3	53.3	14
	B	052815-2	1.58	2.70	2.75	3.03	3.42	2.80	15	72.4	114.0	142.9	175.4	202.1	144.7	15
BC	C	052615-1A	1.58	1.71	1.76	1.89	2.53	1.89	9	34.9	50.0	56.7	65.8	83.8	58.5	9
	D	052615-2	0.14	0.54	0.62	0.67	0.78	0.57	11	62.9	74.6	105.8	110.7	164.2	99.6	11

Relative K_{IC*} decreases between background and fault-proximal samples obtained from the retrograde Box Canyons site, whereas the silicified fault proximal material at Dixie Comstock is substantially tougher than the background sample. Subcritical index generally increases with alteration at both sites, although overlap between maximum and minimum SCI values makes these trends less robust. K-V curves for the two sites show a different velocity pattern between background and more altered rock (Figure 5). K-V plots from both sites span the same calculated subcritical fracture growth velocities (~10^{-5} to 10^{-9} m/s), but they record propagation at different stress intensities. Fracture propagation in silicified material (B) requires *greater* K_I for all velocities. Increasing alteration and damage in fault proximal material from the Box Canyons (D) corresponds to fracture propagation at *reduced* K_I.

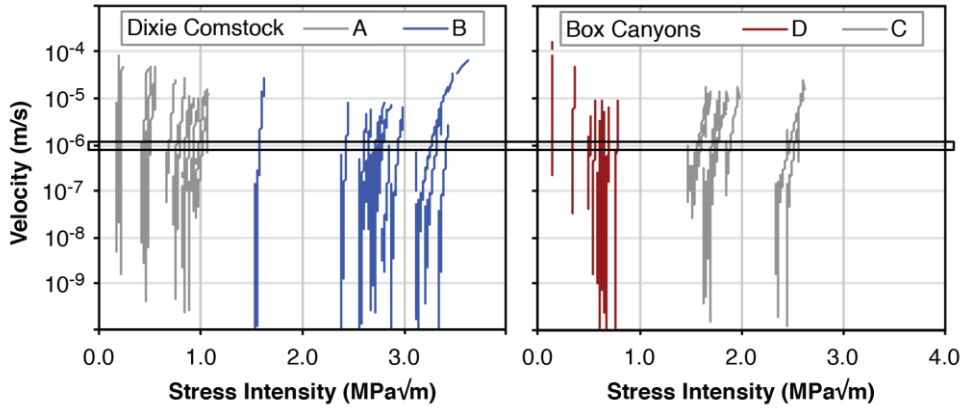

Figure 5. Mode-I stress intensity (K_I) and fracture growth velocity (V) for background material (gray) and fault proximal material (blue, red) at Dixie Comstock and Box Canyons sites. Relative stress intensity K_{IC*} is measured at calculated fracture propagation velocities of 10^{-6} m/s (double line).

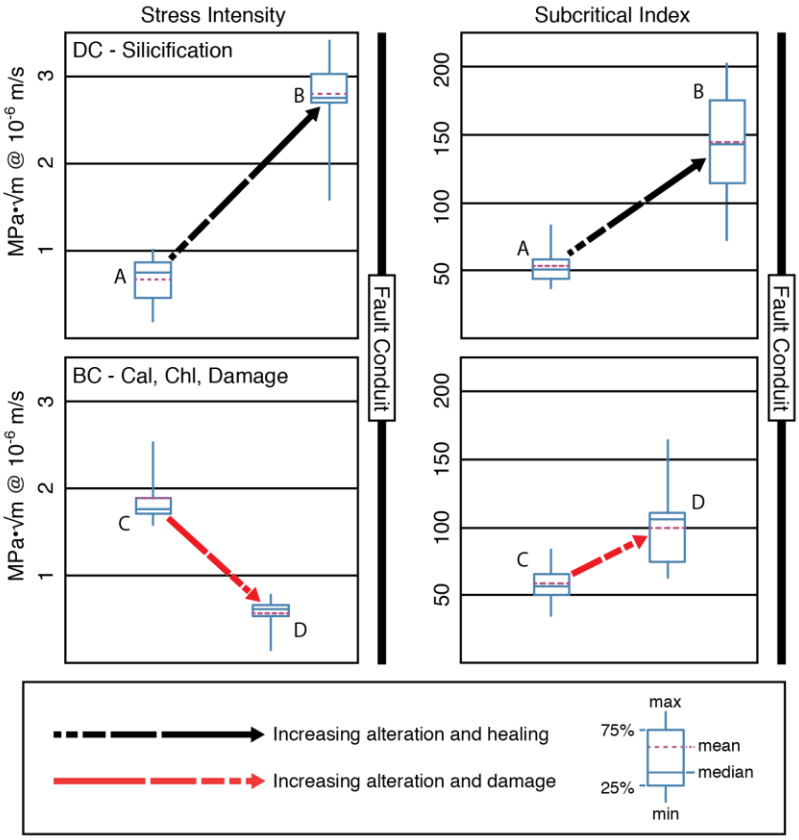

Figure 6. K_{IC*} and SCI in fault-proximal and background samples in different hydrothermal settings. In the retrograde setting, damage dominates and the material becomes mechanically weaker. In areas dominated by mineralization and healing, we

observe an increase in material toughness. SCI increases in fault proximal material at both sites, but this response may arise from different underlying phenomena.

6. DISCUSSION

We observe significant variation in relative stress intensity at calculated fracture propagation velocities of 10^{-6} m/s between background and more altered, fault-conduit proximal material at both locations (Figure 6). In the Box Canyons, where the compositional contrast is dominated by selective alteration of mafic minerals, some alteration of feldspar, damage, and an associated increase in microstructural complexity, we see a reduction in relative stress intensity. By contrast, silicification at Dixie Comstock results in a large increase in relative stress intensity compared to background material (mean of 2.8 vs 0.67 MPa√m). The relative stress intensity we measured in silicified material is higher than relatively unaltered diorite at the Box Canyons site and higher than reported fracture toughness values for unaltered granite (1.74-2.5 MPa√m; Atkinson, 1984) and andesite (1.69 MPa√m; Nara et al., 2012).

Swanson (1984) described the physical meaning of changing subcritical indices with particular clarity: "Large values of *n* are produced in samples with cracks that are rapidly arrested". At both sites, basic statistical measurements of subcritical index increase with increasing alteration. In damaged material, grain size reduction and the introduction of microstructural complexity are consistent with an observed increase in subcritical index in other types of rocks (e.g. Atkinson, 1984). The elevated subcritical index in the silicified material (mean of 144) is similar to those measured for fine-grained basalt (100-170, Swanson, 1984) but distinctly higher than values reported for fine-grained novaculite (~25, Atkinson, 1980), perhaps due to grain size heterogeneity and complexity in our silicified sample. Overall, our measured subcritical indices are consistent with at least one reported range for rocks (70-170; Swanson, 1984).

The distribution of chemical and mechanical alteration and damage around hydrothermal systems and the associated contrast in fracture-mechanical properties that we observe likely impacts the natural development of fault-fracture conduit geometry. In deep portions of hydrothermal systems that are dominated by dissolution, we expect comparatively narrow fault-fracture conduits due to localized reduction of fracture strength. By contrast, strengthening in silicified conduits may enhance distributed fracturing in adjacent material, contributing to large fractured volumes and distributed alteration in shallow portions of the system. Additionally, knowledge of the fracture mechanical properties of different alteration assemblages may help in the design of reservoir stimulation strategies in traditional and enhanced geothermal systems (e.g. Zhao, 1994). Modeling efforts in support of hydrothermal development projects have long considered coupled chemical and mechanical interactions, and complexities arising from fractured media (see review in Ghassemi, 2012). However, our results offer some of the first experimental measurements of fracture mechanical properties of the types of chemically and mechanically altered rock commonly encountered in hydrothermal systems.

7. CONCLUSIONS

We conducted double torsion fracture mechanical measurements on two pairs of variably altered and damaged rocks to describe the impact of alteration and deformation on fracture mechanical properties in fault-hosted hydrothermal systems. Samples ranged from relatively unaltered diorite, to moderately chlorite ±calcite ±hematite ±sericite altered and pervasively damaged diorite and gabbro, to near complete replacement of gabbro by massive silicification.

Our tests indicate that alteration influences fracture mechanical properties to varying extent. Samples containing moderate alteration and unhealed damage are mechanical weak, whereas silicification is associated with high relative K_{IC*} and SCI. We conclude that changes in mechanical properties are related to the dominant alteration mechanism rather than the degree of alteration. A key control on fracture mechanical behavior, including subcritical fracture growth, of altered rocks is the prevalence of existing damage, in the form of microfractures and dissolution, versus mineral precipitation and healing.

These results have implications for the geometry of naturally occurring hydrothermal systems and practical applications in operating geothermal fields. Based on the alteration assemblages that we tested, the mechanical contrast between fault zone and host appears to reverse between deep and shallow portions of the system: precipitation in shallow portions of the system may seal and strengthen fault-fracture conduits, while damage and dissolution at depth may contribute to mechanical localization of fault-fracture conduits. When designing hydrothermal stimulations, it follows that regions of moderate alteration and pre-existing damage may be more prone to failure than pervasively silicified intervals. Additionally, subcritical fracture growth is not equal across all rock types, and may occur at lower relative stress intensities in background, off-fault material. This relationship should be considered in geomechanical models used to design well stimulations and forecast the duration of fracture-hosted hydrothermal circulation.

ACKNOWLEDGMENTS

This work was funded by grants from The GDL Foundation, The Geothermal Resources Council, and The AAPG Foundation. Additional support was provided by The Jackson School of Geosciences and The Fracture Research and Application Consortium at The University of Texas at Austin. Laboratory assistance was provided by Donnie Brooks, Xiaofeng Chen, and Jonathan Major. Owen Callahan is supported by a Powers Graduate Fellowship at The University of Texas at Austin.

REFERENCES

Anderson, O.L., and Grew, P.C., 1977, Stress corrosion theory of crack propagation with applications to geophysics: Review of Geophysics and Space Physics, v. 15, n. 1, p. 77-104

Anderson, T.R., and Fairley, J.P., 2008, Relating permeability to the structural setting of a fault-controlled hydrothermal system in southeast Oregon, USA: Journal of Geophysical Research, v. 113, n. B5.

Atkinson, B.K., 1979, A fracture mechanics study of subcritical tensile cracking of quartz in wet environments: Pure and Applied Geophysics, v. 117, p. 1011-1024

Atkinson, B.K., 1980, Stress corrosion and the rate-dependent tensile failure of a fine-grained quartz rock: Tectonophysics, v. 65, p. 281-290.

Atkinson, B.K., 1984, Subcritical crack growth in geological materials: JGR, v. 89, n. B6, p. 4077

Brantut, N., Heap, M.J., Meredith, P.G., and Baud, P., 2013, Time-dependent cracking and brittle creep in crustal rocks: A review: Journal of Structural Geology, v. 52, p. 17-43.

Bruhn, R.L., Parry, W.T., Yonkee, W.A., and Thompson, T., 1994, Fracturing and hydrothermal alteration in normal fault zones: Pure and Applied Geophysics, v. 142, n. 3/4, p. 609-644.

Chen, X., Eichhubl, P., Olson, J., in review, Effect of water on subcritical fracture properties of Woodford Shale, Journal of Geophysical Research: Solid Earth.

Cox, S.F., Knackstedt, M.A., and Braun, J., 2001, Principles of structural control on permeability and fluid flow in hydrothermal systems, in Richards, J. P., and Tosdal, R. M., eds., Structural Controls on Ore Genesis, Volume 14: Littleton, Colorado, Society of Economic Geologist, p. 1-24.

Curewitz, D., and Karson, J.A., 1997, Structural settings of hydrothermal outflow: Fracture permeability maintained by fault propagation and interaction: Journal of Volcanology and Geothermal Research, v. 79, n. 3, p. 149-168.

Davatzes, N.C., and Hickman, S.H., The feedback between stress, faulting, and fluid flow: lessons from the Coso Geothermal Field, CA, USA, in Proceedings World Geothermal Congress, Bali, Indonesia, 25-29 April 2010, p. 1-15.

Dempsey, D.E., Rowland, J.V., Zyvoloski, G.A., and Archer, R.A., 2012, Modeling the effects of silica deposition and fault rupture on natural geothermal systems: Journal of Geophysical Research. Solid Earth, v. 117, n. 5.

Eichhubl, P., and Boles, J.R., 2000, Focused fluid flow along faults in the Monterey Formation, coastal California. Geological Society of America Bulletin, v. 112, p. 1667-1679.

Eichhubl, P., Davatzes, N.C., and Becker, S.P., 2009, Structural and diagenetic control of fluid migration and cementation along the Moab fault, Utah: AAPG Bulletin, v. 93, n. 5, p. 653-681.

Eichhubl, P., Taylor, W.L., Pollard, D.D., and Aydin, A., 2004, Paleo-fluid flow and deformation in the Aztec Sandstone at the Valley of Fire, Nevada; Evidence for the coupling of hydrogeologic, diagenetic, and tectonic processes: Geological Society of America Bulletin, v. 116, n. 9-10, p. 1120-1136.

Evans, A.G., 1972, A method for evaluating the time-dependent failure characteristics of brittle materials - and its application to polycrystalline alumina: Journal of Materials Science, v. 7, p. 1137-1146.

Facca, G., and Tonani, F., 1967, The self-sealing geothermal field: Bulletin Volcanologique, v. 30, n. 1, p. 271-273

Faulds, J.E., Coolbaugh, M.F., Vice, G.S., and Edwards, M.L., 2006, Characterizing structural controls of geothermal fields in the northwestern Great Basin: a progress report: Geothermal Resources Council Transactions, v. 30, p. 69-76.

Finzi, Y., Hearn, E.H., Lyakhovsky, V., and Gross, L., 2011, Fault-zone healing effectiveness and the structural evolution of strike-slip fault systems: Geophysical Journal International, v. 186, n. 3, p. 963-970

Ghassemi, A., 2012, A Review of Some Rock Mechanics Issues in Geothermal Reservoir Development: Geotechnical and Geological Engineering, v. 30, no. 3, p. 647-664.

Gherardi, F., Xu, T., and Pruess, K., 2007, Numerical modeling of self-limiting and self-enhancing caprock alteration induced by CO2 storage in a depleted gas reservoir: Chemical Geology, v. 244, no. 1-2, p. 103-129.

Haas, J.L., Jr., 1971, The effect of salinity on the maximum thermal gradient of a hydrothermal system at hydrostatic pressure: Economic Geology and the Bulletin of the Society of Economic Geologists, v. 66, n. 6, p. 940-946.

Hedderly-Smith, D.A., 1997, A geochemical examination of the Dixie Valley fault, Nevada: Implications for the propagation and behavior of seismogenic normal faults. PhD: The University of Utah, 322 p.

Laubach, S.E., Eichhubl, P., Hilgers, C., and Lander, R.H., 2010, Structural diagenesis: Journal of Structural Geology, v. 32, n. 12, p. 1866-1872.

Micklethwaite, S., Sheldon, H.A., and Baker, T., 2010, Active fault and shear processes and their implications for mineral deposit formation and discovery: Journal of Structural Geology, v. 32, n. 2, p. 151-165.

Nara, Y., Morimoto, K., Hiroyoshi, N., Yoneda, T., Kaneko, K., and Benson, P. M., 2012, Influence of relative humidity on fracture toughness of rock: implications for subcritical crack growth: International Journal of Solids and Structures, v. 49, p. 2471-2481.

Olson, J.E., 1993, Joint pattern development: effects of subcritical crack growth and mechanical crack interaction: Journal of Geophysical Research, v. 98, n. B7, p. 12,251-212,265.

Olson, J.E., 2004, Predicting fracture swarms - the influence of subcritical crack growth and the crack-tip process zone on joint spacing in rock: Geological Society, London, Special Publications, v. 231, n. 1, p. 73-88.

Ord, A., Hobbs, B.E., and Lester, D.R., 2012, The mechanics of hydrothermal systems: I. Ore systems as chemical reactors: Ore Geology Reviews, v. 49, p. 1-44.

Parry, W.T., Hedderly-Smith, D., and Bruhn, R.L., 1991, Fluid inclusions and hydrothermal alteration on the Dixie Valley Fault, Nevada: Journal of Geophysical Research, v. 96, n. B12, p. 19733.

Pletka, B.J., Fuller, E.R., Jr., and Koepke, B.G., 1979, An evaluation of double-torsion testing - experimental, in Freiman, S. W., ed., Fracture Mechanics Applied to Brittle Materials, ASTM STP 678, American Society for Testing and Materials, p. 19-37.

Pletka, B.J., and Wiederhorn, S.M., 1978, Subcritical crack growth in glass-ceramics, *in* Fracture Mechanics of Ceramics, v. 4, Bradt, R.C., Hasselman, D.P.H., and Lange, F.F., eds., Plenum Press, New York, p. 745-759.

Rijken, M.C.M., 2005, Modeling naturally fractured reservoirs: from experimental rock mechanics to flow simulation. Ph.D.: The University of Texas at Austin, 239 p.

Rudnicki, J.W., 1980, Fracture mechanics applied to the earth's crust: Annual Review of Earth and Planetary Sciences, v. 8, p. 489-525.

Sornette, D., 1999, Earthquakes: From chemical alteration to mechanical rupture: Physics Reports, v. 313, n. 5, p. 237-292. Sites

Swanson, E.L., 1984, Subcritical crack growth and other time- and environment-dependent behavior in crustal rocks. JGR, v. 89, 4137-4152

Vikre, P.G., 1993, Gold mineralization and fault evolution at the Dixie Comstock Mine, Churchill County, Nevada: Economic Geology, v. 89, n. 4, p. 707-719.

Williams, D.P., and Evans, A.G., 1973, A simple method for studying slow crack growth: JTEVA, v. 1, n. 4, p. 264-270.

Wyering, L.D., Villeneuve, M.C., Wallis, I.C., Siratovich, P.A., Kennedy, B.M., Gravley, D.M., and Cant, J.L., 2014, Mechanical and physical properties of hydrothermally altered rocks, Taupo Volcanic Zone, New Zealand: Journal of Volcanology and Geothermal Research, v. 288, p. 76-93.

Zhao, J., 1994, Geothermal testing and measurements of rock and rock fractures: Geothermics, v. 23, no. 3, p. 215-231.